Inorg. Chem. **2007**, *46*, 2735–2743

Inorganic Chemistry
Article

Di(μ-oxo) Binuclear Manganese(III,IV) Poly(bipyridyl) Complexes Bearing Four Ruthenium(II) Photoactive Units: Synthesis, Characterization, and Photoinduced Electron-Transfer Properties

Sophie Romain, Jean-Claude Leprêtre,[†] Jérôme Chauvin, Alain Deronzier,* and Marie-Noëlle Collomb*

*Laboratoire d'Electrochimie Organique et de Photochimie Rédox, Université Joseph Fourier,
UMR CNRS 5630, Institut de Chimie Moléculaire de Grenoble, FR CNRS 2607, BP 53, 38041
Grenoble Cedex 9, France*

Received December 26, 2006

In order to model the photoinduced electron-transfer reactions from the manganese cluster to the photoactive P_{680} chlorophylls in photosystem II, three heterohexanuclear complexes, $[Mn_2^{III,IV}O_2\{Ru^{II}(bpy)_2(L_n)\}_4]^{11+}$ [bpy = 2,2′-bipyridine, $n = 2$ (**1a**), 4 (**1b**), 6 (**1c**)], in which one $Mn^{III,IV}(\mu\text{-}O)_2$ center is covalently linked to four $Ru^{II}(bpy)_3$-like moieties by bridged bis(bipyridine) L_n ligands, have been synthesized and characterized. The electrochemical, photophysical, and photochemical properties of these complexes have been investigated in CH_3CN. The cyclic voltammograms and rotating-disk electrode curves of the three complexes show the presence of two very close successive reversible oxidation processes corresponding to the $Mn_2^{III,IV}/Mn_2^{IV,IV}$ and Ru^{II}/Ru^{III} redox couples (estimated $E_{1/2} \approx 0.82$ and 0.90 V, respectively). The lower potential of the $Mn_2^{III,IV}$ subunit compared to those of the Ru^{II} moieties indicates that the Ru^{III} species can act as an efficient oxidant toward the $Mn_2^{III,IV}$ core. The two oxidized forms of the complexes $[Mn_2^{IV,IV}O_2\{Ru^{II}(bpy)_2(L_n)\}_4]^{12+}$ (**2a**–**c**) and $[Mn_2^{IV,IV}O_2\{Ru^{III}(bpy)_2(L_n)\}_4]^{16+}$ (**3a**–**c**) obtained in good yields (>90% for **2a**–**c** and >85% for **3a**–**c**) by sequential electrolyses are very stable. Photophysical studies show that the ^{3}MLCT excited state of the $Ru(bpy)_3$ centers is moderately quenched by the $Mn_2^{III,IV}(\mu\text{-}O)_2$ core (15–25% depending on the length of the bridging alkyl chain). Nevertheless, this energy transfer can be easily short-circuited in the presence of an external irreversible electron acceptor like the (4-bromophenyl)diazonium cation, by an electron transfer leading, in a stepwise fashion, to the stable one- and five-electron-oxidized species **2a**–**c** and **3a**–**c**, respectively, also in good yields, under continuous irradiation of the solutions. Electro- and photoinduced oxidation experiments have been followed by UV–visible and electron paramagnetic resonance spectroscopy.

Introduction

The biological generation of dioxygen from water during photosynthesis occurring through photosystem II (PSII) is one of the most important and fundamental photochemical processes in nature.[1] In PSII, the oxidation of water to molecular oxygen is initiated by the absorption of a photon by the photoactive P_{680} chlorophylls. An electron is then transferred from the excited P_{680}* to a series of electron acceptors. Thereafter, P_{680}^+ extracts one electron from the oxygen-evolving complex (OEC), a cubane-like Mn_4O_xCa cluster, via a tyrosine residue (tyrosine$_Z$). After four consecutive photoinduced electron-transfer reactions, the four-electron-oxidized OEC recovers all four electrons in one step by oxidizing two water molecules to molecular oxygen.[2]

In recent years, several Ru−Mn bimetallic complexes have been synthesized, with the aim of modeling these photoinduced electron-transfer reactions from the Mn cluster to

---

* To whom correspondence should be addressed. E-mail: alain.deronzier@ujf-grenoble.fr (A.D.), marie-noelle.collomb@ujf-grenoble.fr (M.-N.C.).

[†] Present address: LEPMI/ELSA/ENSEEG, Domaine Universitaire, 1130 rue de la piscine, BP 75, 38042 Saint Martin d'Hères, France.

(1) (a) Photosynthetic water oxidation: Special Dedicated Issue. Nugent, J., Ed. *Biochim. Biophys. Acta* **2001**, *1503*, 1. (b) Barber, J. *Q. Rev. Biophys.* **2003**, *36*, 71.

(2) (a) Ferreira, K. N.; Iverson, T. M.; Maghlaoui, K.; Barber, J.; Iwata, S. *Science* **2004**, *303*, 1831. (b) Loll, B.; Kern, J.; Saenger, W.; Zouni, A.; Biesiadka, J. *Nature* **2005**, *438*, 1040. (c) Haumann, M.; Liebisch, P.; Müller, C.; Barra, M.; Grabolle, M.; Hau, H. *Science* **2005**, *310*, 1019.

10.1021/ic0624726 CCC: $37.00

P_{680}^{+}.[3,4] One of the main strategies used involves the covalent coupling of a photoactive ruthenium(II) tris(bipyridine) [$Ru^{II}(bpy)_3$; bpy = 2,2′-bipyridine] like unit, which mimics the function of the P_{680} chlorophyll photosensitizer, to some redox-active mono-,[5] bi-,[6] and trinuclear[4a] Mn moieties, usually in low oxidation states (II or III), that are intended to mimic the natural Mn_4O_xCa complex. Some of these compounds include a substituted tyrosine between the Ru and Mn moieties, which functions as a redox-active intermediate, in the manner of the natural system.[4,6] In all of these heterobimetallic complexes, light-induced intramolecular electron transfer from the Mn moiety to the photooxidized $Ru^{III}(bpy)_3^{3+}$ center has been observed in the presence of an external electron acceptor such as viologen in acetonitrile. Complexes with a multinuclear Mn core are observed to have faster electron-transfer rate constants ($>10^7$ s^{-1}) compared to mononuclear ones. Most of these studies were conducted using flash photolysis, with only a few of them describing the photoinduced oxidation of the Mn center under prolonged irradiation.[6b] In the best case, three electrons were transferred, in a stepwise fashion, from a dinuclear $Mn_2^{II,II}$ core to the linked Ru center, leading to the partial formation of the oxo-bridged $Mn_2^{III,IV}$ core when the experiments are carried out in the presence of water.

Chart 1

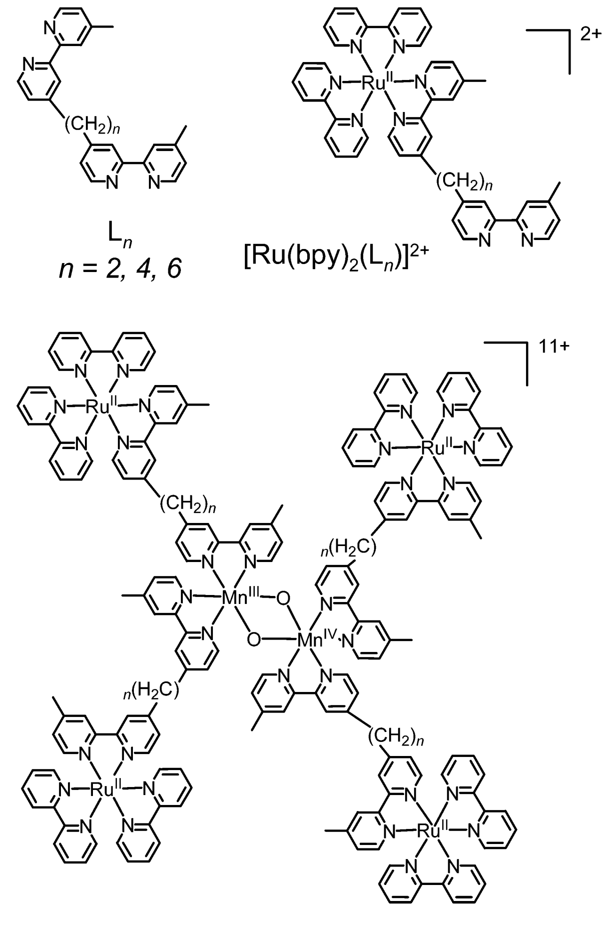

L_n
$n = 2, 4, 6$

$[Ru(bpy)_2(L_n)]^{2+}$

$[Mn_2O_2\{Ru(bpy)_2(L_n)\}_4]^{11+}$
1a ($n = 2$)
1b ($n = 4$)
1c ($n = 6$)

On the other hand, among the Mn−Ru complexes that have been prepared, there is only one example of a structure containing high-valent μ-oxo-bridged Mn centers that is structurally close to the natural Mn_4O_xCa cluster. This is the $Mn_2^{IV,IV}(\mu\text{-}O)_2$ complex $[Mn_2O_2(\text{bis-Ru-tacn})]^{6+}$, in which bis-Ru-tacn is a bis(triazacyclononane)-type macrocycle covalently bonded to two $Ru^{II}(bpy)_3$-like units.[4b] However, this complex cannot be photooxidized because the Mn ions are already in their highest accessible oxidation state. Analogous molecules containing Mn ions of lower oxidation states are difficult to prepare; recent attempts to prepare and isolate the $Mn_2^{III,IV}(\mu\text{-}O)_2$ complex $[Mn_2O_2(\text{Ru-terpy})_2(H_2O)_2]^{7+}$ using a terpyridyl ligand covalently linked to a $Ru(bpy)_3$ unit (denoted Ru-terpy) with a significant yield were unsuccessful.[7] We have recently demonstrated that a series of $Mn_2^{III,IV}(\mu\text{-}O)_2$ complexes, $[Mn_2^{III,IV}O_2\{Ru^{II}(bpy)_2(L_n)\}_4]^{11+}$ [$n = 2$ (**1a**), 4 (**1b**), 6 (**1c**); Chart 1), which bear four $Ru^{II}(bpy)_3$-type units via bis(bipyridinyl) L_n ligands, can be in situ prepared by electrochemical or photoinduced oxidation of corresponding tetranuclear complexes $[\{Ru^{II}(bpy)_2(L_n)\}_3Mn^{II}]^{8+}$.[8] We report here a straightforward chemical synthesis of **1a**−**c**, their characterization, and their redox and photophysical properties. The stability of the two oxidized forms of the complexes, $[Mn_2^{IV,IV}O_2\{Ru^{II}(bpy)_2(L_n)\}_4]^{12+}$ (**2a**−**c**) and $[Mn_2^{IV,IV}O_2\{Ru^{III}(bpy)_2(L_n)\}_4]^{16+}$ (**3a**−**c**), corresponding to a one- and five-electron oxidation of **1a**−**c**, respectively, is also investigated by exhaustive electrolyses. In addition, we find that the photoinduced selective oxidation of the Mn core of **1a**−**c** to give the **2a**−**c** species

---

(3) (a) Sun, L.; Hammarström, L.; Akermark, B.; Styring, S. *Chem. Soc. Rev.* **2001**, *30*, 36. (b) Hammarström, L. *Curr. Opin. Chem. Biol.* **2003**, *7*, 666 and references cited therein.

(4) (a) Burdinski, D.; Wieghardt, K.; Steenken, S. *J. Am. Chem. Soc.* **1999**, *121*, 10781. (b) Burdinski, D.; Bothe, E.; Wieghardt, K. *Inorg. Chem.* **2000**, *39*, 105.

(5) (a) Sun, L.; Hammarström, L.; Norrby, T.; Berglund, H.; Davydov, R.; Andersson, M.; Börje, A.; Korall, P.; Philouze, C.; Almgren, M.; Styring, S.; Akermark, B. *Chem. Commun.* **1997**, 607. (b) Sun, L.; Berglund, H.; Davydov, R.; Norrby, T.; Hammarström, L.; Korall, P.; Börje, A.; Philouze, C.; Berg, K.; Tran, A.; Andersson, M.; Stenhagen, G.; Martensson, J.; Almgren, M.; Styring, S.; Akermark, B. *J. Am. Chem. Soc.* **1997**, *119*, 6996. (c) Berglund-Baudin, H.; Sun, L.; Davidov, R.; Sundahl, M.; Styring, S.; Akermark, B.; Almgren, M.; Hammarström, L. *J. Phys. Chem. A* **1998**, *102*, 2512. (d) Berg, K. E.; Tran, A.; Raymond, M. K.; Abrahamsson, M.; Wolny, J.; Redon, S.; Andersson, M.; Sun, L.; Hammarström, L.; Toftlund, H.; Akermark, B. *Eur. J. Inorg. Chem.* **2001**, 1019. (e) Abrahamsson, M. L. A.; Baudin, H. B.; Tran, A.; Philouze, C.; Berg, K. E.; Raymond-Johansson, M. K.; Sun, L.; Akermark, B.; Styring, S.; Hammarström, L. *Inorg. Chem.* **2002**, *41*, 1534.

(6) (a) Sun, L.; Raymond, M. K.; Magnuson, A.; LeGourriérec, D.; Tamm, M.; Abrahamsson, M.; Kenéz, P. H.; Martensson, J.; Stenhagen, G.; Hammarström, L.; Styring, S.; Akermark, B. *J. Inorg. Biochem.* **2000**, *78*, 15. (b) Huang, P.; Magnuson, A.; Lomoth, R.; Abrahamsson, M.; Tamm, M.; Sun, L.; van Rotterdam, B.; Park, J.; Hammarström, L.; Akermark, B.; Styring, S. *J. Inorg. Biochem.* **2002**, *91*, 159. (c) Johansson, A.; Abrahamsson, M.; Magnuson, A.; Huang, P.; Martensson, J.; Styring, S.; Hammarström, L.; Sun, L.; Akermark, B. *Inorg. Chem.* **2003**, *42*, 7502.

(7) Wolpher, H.; Huang, P.; Borgström, M.; Bergquist, J.; Styring, S.; Sun, L.; Akermark, B. *Catal. Today* **2004**, *98*, 529.

(8) Romain, S.; Baffert, C.; Dumas, S.; Chauvin, J.; Leprêtre, J.-C.; Daveloose, D.; Deronzier, A.; Collomb, M.-N. *Dalton Trans.* **2006**, *48*, 5691.

can be achieved with a good yield in the presence of a sacrificial oxidative quencher.

Experimental Section

Materials and General Procedures. Acetonitrile (CH_3CN; Rathburn, HPLC grade) and tetra-*n*-butylammonium perchlorate (TBAP; Fluka) were used as received and stored under an argon atmosphere in a dry glovebox (Jaram). 2,6-Dimethylpyridine [lutidine (98%, Fluka)] was distilled over CaH_2 prior use. *tert*-Butyl hydroperoxide (^{t}BuOOH; 70% in water, Fluka) was used as received. ^{1}H NMR spectra were recorded on a Bruker AC 250 spectrometer. Elemental analyses were performed by the Service Central d'Analyse du CNRS at Vernaison (France).

Electrospray Ionization Mass Spectrometry (ESI-MS). ESI-MS experiments were performed on a triple-quadrupole mass spectrometer Quattro II (Micromass, Altrincham, U.K.). The ESI source was heated to 80 °C. The sampling cone voltage was set within the range 4−20 V according to the complex studied. Complexes in solution (1−2 mg mL^{-1} in CH_3CN) were injected using a syringe pump at a flow rate in the range 5−10 μL min^{-1}. The electrospray probe (capillary) voltage was optimized in the range 2.9−5 kV for positive-ion electrospray.

Electrochemistry. Electrochemical measurements were performed as previously detailed.[9,10] All potentials reported here were referenced to an Ag/10 mM $AgNO_3$ reference electrode in CH_3CN + 0.1 M TBAP. Potentials referred to that system can be converted to the ferrocene/ferrocenium redox system by subtracting 87 mV.

Spectroscopy. X-band electron paramagnetic resonance (EPR) spectra were recorded with a Bruker ESP 300 E spectrometer at 100 K, with the following parameters: microwave 1 mW, modulation amplitude 0.197 G, time constant 327.68 ms, scan rate 1342 s, scan width 8 G, and modulation frequency 100 kHz. UV−visible absorption spectra were obtained using Cary 50 and Cary 100 absorption spectrophotometers on 1 mm and 1 cm path length quartz cells. For emission experiments, samples were prepared in a glovebox and contained in a 1 cm path length quartz cuvette. Samples were maintained in aerobic conditions with a Teflon cap. Emission spectra were recorded at room temperature on a Photon Technology International SE-900M spectrofluorimeter. The excitation wavelength was 450 nm, and spectra were recorded from 500 to 850 nm and corrected for the photomultiplier response. Emission quantum yields ϕ_L were determined at 25 °C in deoxygenated acetonitrile solutions with $[Ru(bpy)_3](PF_6)_2$ used as a standard ($\phi_L^{ref} = 0.062$)[11] and following the methodology already presented.[12] Emission lifetimes were measured with a 4 ns pulsed N_2 laser $\lambda = 337$ nm (optilas VSL-337ND-S) and recorded at $\lambda = 600$ nm using a monochromator and a photomultiplicator tube (Hamamatsu R928) coupled with an ultrafast oscilloscope (Tektronix TDS 520A). The τ values were determined by the average of three different experiments; the margin of error for τ was estimated to be less than 10%.

Continuous Irradiations. Irradiation experiments were performed using a medium-pressure mercury lamp (Oriel 66901; 250 W) whose UV and IR radiations were filtered with a large band-pass filter centered at around $\lambda = 560$ nm (irradiation between 410 and 710 nm), as previously detailed.[9,10] Using these filters and a diaphragm, the samples received around 8 mW at 416 nm. The same experiments were conducted with a xenon lamp, under similar irradiation power, equipped with the following accessories: T2 and T_a2 MTO filters to avoid IR light and a 3-73 Corning filter to select the visible region ($\lambda > 410$ nm)[13] have led to similar experimental results. For these experiments, all of the solutions were prepared in a glovebox under argon, in a 1 cm path length quartz cuvette, which was maintained under anaerobic conditions with a Teflon cap. The solutions contained a mixture of **1a**−**c** (∼0.45 mM) and ArN_2^+ (15 mM). Under these conditions, the concentration of ArN_2^+ can be considered to be constant during the experiments. Photooxidation experiments were followed by UV−visible spectroscopy.

The quantum yield of the formation of **2a** measured after continuous irradiation at 436 nm, performed with a 250 W mercury lamp (Oriel 66901). The desired mercury emission line was isolated using band-pass filters (Oriel 5645). The quantum yield was determined by actinometry at the wavelength of the maximum absorption of the $Mn_2^{III,IV}(O)_2$ core (680 nm), by comparing the absorption of the sample after and before irradiation and using the quantum yield formation of $[Ru^{III}(bpy)_3]^{3+}$ in the system $[Ru^{II}(bpy)_3]^{2+}/ArN_2^+$ as a reference (quantum yield = 0.34).[14] Samples were prepared with the same absorbance (Abs = 2) at 454 nm, and the conversion was fixed at less than 20%. Taking into account the weak variation of the absorbance at this wavelength, this experiment was repeated several times to give an average quantum yield following eq 1.

$$\phi_F^S = \phi_F^{ref}\left(\frac{(\Delta DO)^S_{680\ nm}}{(\Delta DO)^{ref}_{454\ nm}}\right)_{t,\lambda_{irr}=436\ nm} \quad (1)$$

Synthesis of the Diazonium Salt. (4-Bromophenyl)diazonium tetrafluoroborate p-$BrC_6H_4N_2(BF_4)$ [$ArN_2(BF_4)$] was synthezised as described previously.[14]

Synthesis of Ligands L_n and $[Ru^{II}(bpy)_2(L_n)](ClO_4)_2$. The ligands 1,2-bis[4-(4′-methyl-2,2′-bipyridinyl)]ethane (L_2), 1,2-bis-[4-(4′-methyl-2,2′-bipyridinyl)]butane (L_4), 1,2-bis[4-(4′-methyl-2,2′-bipyridinyl)]hexane (L_6), and the corresponding $[Ru^{II}(bpy)_2(L_n)](ClO_4)_2$ complexes were synthesized as previously described[9] except that, for the Ru complexes, $NaClO_4$ was used instead of KPF_6 {$[Ru(bpy)_2(L_2)](ClO_4)_2$ (yield: 32%), $[Ru(bpy)_2(L_4)](ClO_4)_2$ (yield: 38%), $[Ru(bpy)_2(L_6)](ClO_4)_2$ (yield: 47%)}.

Caution! *Perchlorate salts of metal complexes with organic ligands are potentially explosive. Only small quantities of these compounds should be prepared, and they should be handled behind suitable protective shields.*

Synthesis of the Complexes $[Mn_2^{III,IV}O_2\{Ru^{II}(bpy)_2(L_n)\}_4](ClO_4)_{11}$ [1a−c$(ClO_4)_{11}$]. $[Mn_2^{III,IV}O_2\{Ru^{II}(bpy)_2(L_2)\}_4](ClO_4)_{11}$ [1a$(ClO_4)_{11}$]. $Mn(ClO_4)_2 \cdot 6H_2O$ (7.2 mg, 19.8 μmol) and 2,6-dimethylpyridine (9.9 μmol) were added to an orange solution of $[Ru^{II}(bpy)_2(L_n)](ClO_4)_2$ (40.1 mg, 39.5 μmol) in CH_3CN (5 mL). After a few minutes of stirring, 0.75 mol equiv of ^{t}BuOOH (14.8 μmol) was added to the mixture. The formation of **1a** was followed by UV−visible spectroscopy with the appearance of the characteristic ligand-to-metal charge-transfer (LMCT) band of the $Mn_2^{III,IV}(\mu\text{-}O)_2$ core at 680 nm. After 5−10 min, this band reached its maximal intensity with a molar absorption coefficient between 580 and 598 M^{-1} cm^{-1}, close to that of $[Mn_2^{III,IV}O_2(dmbpy)_4]^{3+}$ ($\epsilon = 560$ M^{-1} cm^{-1}), attesting to the quantitative formation of the

---

(9) Lombard, J.; Romain, S.; Dumas, S.; Chauvin, J.; Collomb, M.-N.; Daveloose, D.; Deronzier, A.; Leprêtre, J.-C. *Eur. J. Inorg. Chem.* **2005**, 3320.

(10) Baffert, C.; Dumas, S.; Chauvin, J.; Leprêtre, J.-C.; Collomb, M.-N.; Deronzier, A. *Phys. Chem. Chem. Phys.* **2005**, *7*, 202.

(11) Caspar, J. V.; Meyer, T. J. *J. Am. Chem. Soc.* **1983**, *105*, 5583.

(12) Laguitton-Pasquier, H.; Martre, A.; Deronzier, A. *J. Phys. Chem. B* **2001**, *105*, 4801.

(13) Collomb-Dunand-Sauthier, M.-N.; Deronzier, A.; Ziessel, R. *J. Organometal. Chem.* **1993**, *444*, 191.

(14) Cano-Yelo, H.; Deronzier, A. *J. Chem. Soc., Faraday Trans. B* **1984**, *80*, 3011.

complexes. A total of 3 mL of water was then added to this CH_3CN solution. CH_3CN in the solution was then removed under reduced pressure, leading to the formation of an orange precipitate. The crude product was filtered off, washed with water, and dried under air to give 37 mg (yield: 84%) of **1a**(ClO_4)$_{11}$·$12H_2O$ as an orange powder. Complexes $[Mn_2^{III,IV}O_2\{Ru^{II}(bpy)_2(L_4)\}_4](ClO_4)_{11}\cdot 8H_2O$ [**1b**(ClO_4)$_{11}$·$8H_2O$] and $[Mn_2^{III,IV}O_2\{Ru^{II}(bpy)_2(L_6)\}_4](ClO_4)_{11}\cdot 2H_2O$ [**1c**(ClO_4)$_{11}$·$2H_2O$] were prepared according to the same procedure, using 85.9 and 52.4 mg of $[Ru^{II}(bpy)_2(L_n)](ClO_4)_2$, respectively. All of the hexanuclear complexes were found to be very hygroscopic. Because they were isolated as perchlorate salts, they are potentially explosive and difficult to dry. Only **1c**(ClO_4)$_{11}$ was carefully dried under vacuum, giving satisfactory elemental analysis with only two water molecules. The others complexes **1a**(ClO_4)$_{11}$ and **1b**(ClO_4)$_{11}$ exhibit the same degree of purity as that checked by other analytical techniques.

$[Mn_2^{III,IV}O_2\{Ru^{II}(bpy)_2(L_2)\}_4](ClO_4)_{11}\cdot 12H_2O$ [1a(ClO_4)$_{11}$·$12H_2O$]. Elem anal. Calcd for $C_{176}H_{152}N_{32}Ru_4Mn_2Cl_{11}O_{46}\cdot 12H_2O$ (4571.4): C, 46.23; H, 3.88; N, 9.80. Found: C, 46.53; H, 3.98; N, 9.54. ESI-MS: *m*/*z* (%) 2077.45 (0.4) $[M - 2ClO_4]^{2+}$, 1351.91 (10) $[M - 3ClO_4]^{3+}$, 1025.83 (20) $[M - 5ClO_4 - Ru(bpy)_2(L_2)]^{3+}$, 989.23 (15) $[M - 4ClO_4]^{4+}$, 879.08 (15) $[Ru(bpy)_2(L_2)(ClO_4)]^{+}$, 771.27 (8) $[M - 5ClO_4]^{5+}$, 744.55 (60) $[M - 6ClO_4 - Ru(bpy)_2(L_2)]^{4+}$, 626.39 (4) $[M - 6ClO_4]^{6+}$, 575.9 (35) $[M - 7ClO_4 - Ru(bpy)_2(L_2)]^{5+}$, 522.72 (30) $[M - 7ClO_4]^{7+}$, 463 (26) $[M - 8ClO_4 - Ru(bpy)_2(L_2)]^{6+}$, 389.76 (100) $[Ru(bpy)_2(L_2)]^{2+}$. IR (KBr, cm^{-1}): ν 3401 (vs), 1615 (s), 1557 (m), 1483 (m), 1463 (s), 1444 (s), 1419 (s), 1310 (m), 1271 (w), 1243 (m), 1078 (vs), 831 (m), 762 (s), 729 (m), 689 (m), 668 (vw), 658 (vw), 622 (s), 544 (w), 418 (w).

$[Mn_2^{III,IV}O_2\{Ru^{II}(bpy)_2(L_4)\}_4](ClO_4)_{11}\cdot 8H_2O$ [1b(ClO_4)$_{11}$·$8H_2O$; 90 mg, Yield 91%]. Elem anal. Calcd for $C_{184}H_{168}N_{32}Ru_4Mn_2Cl_{11}O_{46}\cdot 8H_2O$ (4611.75): C, 47.92; H, 4.02; N, 9.72. Found: C, 48.10; H, 3.95; N, 9.52. ESI-MS: *m*/*z* (%) 2133.63 (1) $[M - 2ClO_4]^{2+}$, 1389.58 (12) $[M - 3ClO_4]^{3+}$, 1054.20 (8) $[M - 5ClO_4 - Ru(bpy)_2(L_4)]^{3+}$, 1017.23 (30) $[M - 4ClO_4]^{4+}$, 907.09 (10) $[Ru(bpy)_2(L_4)(ClO_4)]^{+}$, 793.78 (9) $[M - 5ClO_4]^{5+}$, 765.44 (95) $[M - 6ClO_4 - Ru(bpy)_2(L_4)]^{4+}$, 644.96 (7) $[M - 6ClO_4]^{6+}$, 592.66 (22) $[M - 7ClO_4 - Ru(bpy)_2(L_4)]^{5+}$, 538.66 (100) $[M - 7ClO_4]^{7+}$, 477.42 (62) $[M - 8ClO_4 - Ru(bpy)_2(L_4)]^{6+}$, 403.91 (73) $[Ru(bpy)_2(L_4)]^{2+}$. IR (KBr, cm^{-1}): ν 3434 (vs), 1615 (s), 1552 (m), 1482 (m), 1463 (s), 1444 (s), 1419 (s), 1311 (m), 1271 (w), 1243 (m), 1088 (vs), 929 (w), 832 (m), 762 (s), 728 (m), 684 (m), 668 (vw), 658 (vw), 620 (s), 535 (w), 419 (w).

$[Mn_2^{III,IV}O_2\{Ru^{II}(bpy)_2(L_6)\}_4](ClO_4)_{11}\cdot 2H_2O$ [1c(ClO_4)$_{11}$·$2H_2O$; 47 mg, Yield 80%]. Elem anal. Calcd for $C_{192}H_{184}N_{32}Ru_4Mn_2Cl_{11}O_{46}\cdot 2H_2O$ (4612.5): C, 49.95; H, 4.10; N, 9.71. Found: C, 50.06; H, 4.25; N, 9.62. ESI-MS: *m*/*z* (%) 2191.01 (80) $[M - 2ClO_4]^{2+}$, 1427.29 (2) $[M - 3ClO_4]^{3+}$, 1045.27 (5) $[M - 4ClO_4]^{4+}$, 935.16 (10) $[Ru(bpy)_2(L_6)(ClO_4)]^{+}$, 817.54 (0.7) $[M - 5ClO_4]^{5+}$, 786.65 (21) $[M - 6ClO_4 - Ru(bpy)_2(L_6)]^{4+}$, 609.49 (30) $[M - 7ClO_4 - Ru(bpy)_2(L_6)]^{5+}$, 491.26 (42) $[M - 8ClO_4 - Ru(bpy)_2(L_6)]^{6+}$, 417.89 (100) $[Ru(bpy)_2(L_6)]^{2+}$. IR (KBr, cm^{-1}): ν 3437 (vs), 1615 (s), 1555 (m), 1483 (m), 1463 (s), 1445 (s), 1421 (s), 1311 (m), 1271 (w), 1243 (m), 1085 (vs), 929 (w), 832 (m), 763 (s), 730 (m), 688 (m), 668 (vw), 658 (vw), 621 (s), 539 (w), 420 (w).

Results and Discussion

Synthesis and Characterization. The three hexanuclear complexes **1a**−**c** have been synthesized by the addition of the two-electron-oxidizing agent ^tBuOOH to a CH_3CN solution containing a mixture of $Mn(ClO_4)_2\cdot 6H_2O$, $[Ru(bpy)_2(L_n)](ClO_4)_2$, and the external base 2,6-dimethylpyridine (denoted B)[15] in the respective mole ratios 0.75:1:2:0.5 (eq 2).

$$2Mn^{2+} + 4[Ru^{II}(bpy)_2(L_n)]^{2+} + {}^1/_2H_2O + B + {}^3/_2{}^tBuOOH \rightarrow [Mn_2^{III,IV}O_2\{Ru^{II}(bpy)_2(L_n)\}_4]^{11+} + BH^+ + {}^3/_2{}^tBuOH \quad (2)$$

The formation of these (μ-O)$_2$ complexes is the result of the one-electron oxidation of the tetranuclear complexes $[\{Ru^{II}(bpy)_2(L_n)\}_3Mn^{II}]^{8+}$ formed in situ (eq 3) into the unstable $[\{Ru^{II}(bpy)_2(L_n)\}_3Mn^{III}]^{9+}$ complexes (eq 4) by analogy with the behavior of $[Mn(L)_3]^{2+}$ [L = bpy, dmbpy, and phen (1,10-phenanthroline)], for which chemical[16] or electrochemical[10,17] oxidation in CH_3CN gives $[Mn_2^{III,IV}O_2(L)_4]^{3+}$.

$$Mn^{2+} + 2[Ru^{II}(bpy)_2(L_n)]^{2+} \rightarrow {}^2/_3[\{Ru^{II}(bpy)_2(L_n)\}_3Mn^{II}]^{8+} + {}^1/_3Mn^{2+} \quad (3)$$

$$[\{Ru^{II}(bpy)_2(L_n)\}_3Mn^{II}]^{8+} \rightarrow [\{Ru^{II}(bpy)_2(L_n)\}_3Mn^{III}]^{9+} + e^- \quad (4)$$

For the oxidation of complexes **1a**−**c** by ^tBuOOH, the protons released during the process are consumed by the chemical oxidant (eq 5) and B, allowing the quantitative formation of the expected complexes following eq 1.

$${}^tBuOOH + 2H^+ + 2e^- \rightarrow {}^tBuOH + H_2O \quad (5)$$

Evidence for the formation of **1a**−**c** has been obtained in situ by UV−visible absorption spectroscopy with the appearance of the characteristic LMCT band (oxo ligands to Mn^{IV}) of the $Mn_2^{III,IV}$ moieties at 680 nm. The poor solubility of these complexes in water as perchlorate salt compared to the byproducts formed, BH^+ and ^tBuOH, has allowed their isolation in pure forms in high yields (see the Experimental Section). The purity of these highly charged cationic hexanuclear complexes was checked by elemental analysis and confirmed by EPR, IR, and UV−visible spectroscopies, by ESI-MS, and by electrochemistry (see below). IR spectra of the compounds exhibit bands in the 750−500 cm^{-1} region, with the typical Mn−O stretching bands of the $\{Mn_2O_2\}$ core in $[Mn_2^{III,IV}O_2(L)_4]^{3+}$ complexes at 684−689 and 728−730 cm^{-1} (688 and 730 cm^{-1} for $[Mn_2^{III,IV}O_2(dmbpy)_4]^{3+}$).[17b] The absorption spectra of **1a**−**c** in CH_3CN correspond to the superimposition of the absorbance of the Ru^{II} and $Mn_2^{III,IV}$ subunits in their respective proportions (4:1) with intense bands at 354 (sh), 396 (sh), 430 (sh), and 454 nm due to the four Ru^{II} subunits and a band at 680 nm arising from the

---

[15] Cauquis, G.; Deronzier, A.; Serve, D.; Vieil, E. *J. Electroanal. Chem.* **1975**, *60*, 205.

[16] Ménage, S.; Collomb-Dunand-Sauthier, M.-N.; Lambeaux, C.; Fontecave, M. *Chem. Commun.* **1994**, 1885.

[17] (a) Morrison, M. M.; Sawyer, D. T. *Inorg. Chem.* **1978**, *17*, 333. (b) Dunand-Sauthier, M.-N. C.; Deronzier, A.; Piron, A.; Pradon, X.; Ménage, S. *J. Am. Chem. Soc.* **1998**, *120*, 5373.

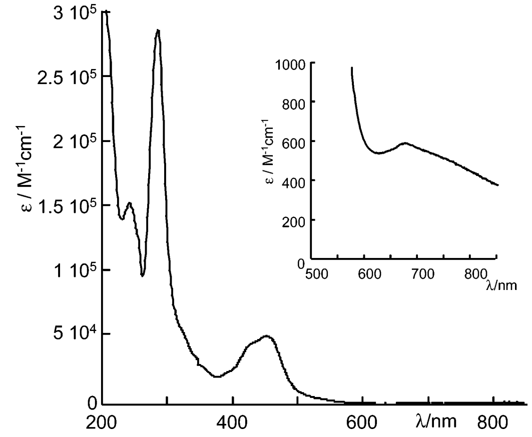

Figure 1. Visible absorption spectra of a solution of **1c** (0.32 mM) in CH_3CN, $l = 0.01$ cm. Inset: $l = 1$ cm.

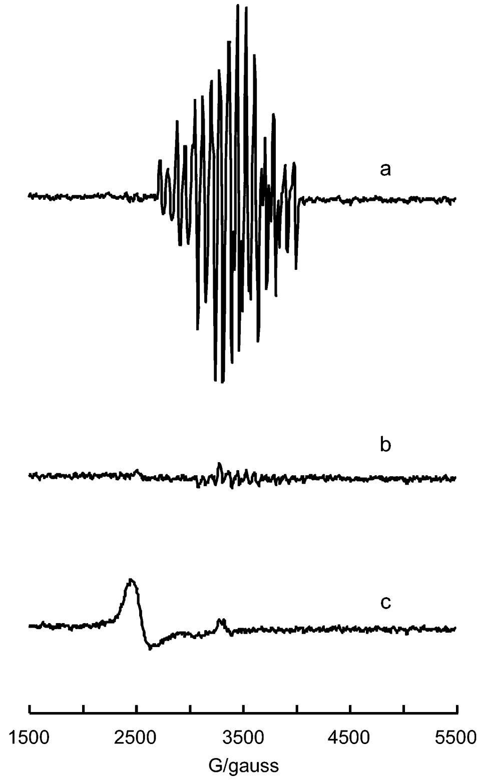

Figure 2. Evolution of the EPR spectrum during electrolyses at 1.0 V of **1c** (0.46 mM) in CH_3CN + 0.1 M TBAP: (a) initial solution; (b) after a one-electron oxidation; (c) after a five-electron oxidation.

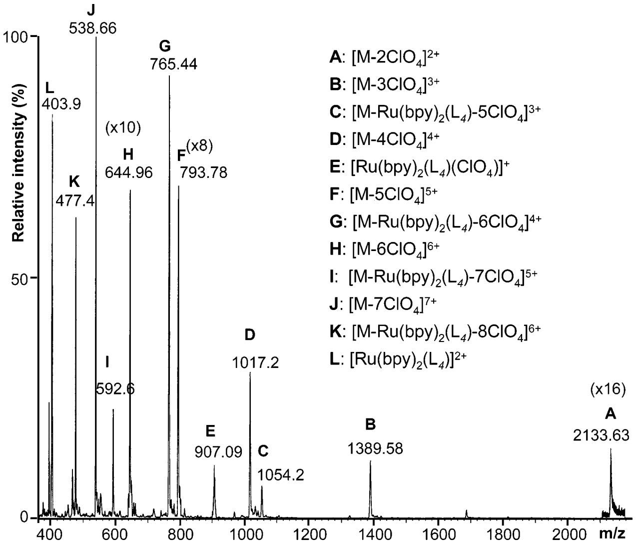

Figure 3. Positive-ion ESI-MS spectrum of a 0.2 mM solution of **1b** in CH_3CN [M = $[Mn_2^{III,IV}O_2\{Ru^{II}(bpy)_2(L_4)\}_4](ClO_4)_{11}$] at a cone voltage of 7 V.

$Mn_2^{III,IV}(\mu\text{-}O)_2$ moiety (oxo to Mn^{IV} charge-transfer band; Figure 1 for **1c** and Table 1).

The molar absorption coefficient of the bands at 680 nm (580−598 M^{-1} cm^{-1}) is slightly higher than that of the corresponding band in $[Mn_2^{III,IV}O_2(dmbpy)_4]^{3+}$ ($\epsilon = 560$ M^{-1} cm^{-1}) because of a slight additional absorption contribution of the Ru^{II} moieties. The other higher energy visible bands (Mn^{IV} d−d transitions) expected for the $Mn_2^{III,IV}$ subunit are masked by the intense Ru^{II} absorptions (Table 1).

EPR and ESI-MS data confirmed that the dinuclear Mn cores were successfully synthesized. The EPR spectrum of each hexanuclear complex in CH_3CN at 100 K shows a clean 16-line signal centered at $g = 2.0$ typical of strongly spin-coupled Mn^{III} and Mn^{IV} ions and displays the absence of mononuclear Mn^{II} impurities in the samples (Figure 2a). The 16-line EPR signal of the three hexanuclear complexes displays splitting patterns and line widths identical with those of $[Mn_2^{III,IV}O_2(dmbpy)_4]^{3+}$,[10] showing that the presence of the four diamagnetic Ru^{II} centers does not significantly perturb the electronic structures of the $Mn_2^{III,IV}(\mu\text{-}O)_2$ cores in the heterobimetallic complexes.

The ESI-MS spectra in the positive mode of 0.2−0.4 mM CH_3CN solutions of **1a**−**c**$(ClO_4)_{11}$ at cone voltages ranging between 4 and 14 V and in the mass range 400−6000 display signals corresponding to the different cationic forms of the complexes [loss of two to seven perchlorate counterions for **1a**,**b**$(ClO_4)_{11}$ and of two to five for **1c**$(ClO_4)_{11}$]. These charged ions are denoted by $[M-nClO_4]^{n+}$, where M represents the molecule (Figure 3 for **1b**). All of these peaks have been assigned in comparison with the isotopic profiles calculated for these formulas. Several molecular peaks corresponding to the successive loss of ClO_4^- anions of **1a**−**c**$(ClO_4)_{11}$, which have lost one $[Ru(bpy)_2(L_n)]^{2+}$ unit, are also observed ($[M-Ru(bpy)_2(L_n)-nClO_4]^{(n-2)+}$). The signals of the monocharged and doubly charged ions of the correlated Ru fragment, $[Ru(bpy)_2(L_n)(ClO_4)]^+$ and $[Ru(bpy)_2(L_n)]^{2+}$, respectively, are also observed. Increasing the cone voltage in the ESI source up to 20 V increases the intensity of the $[M-Ru(bpy)_2(L_n)-nClO_4]^{(n-2)+}$ peaks at the expense of the $[M-nClO_4]^{n+}$ ones.

Electrochemistry and Spectroscopy. The redox potentials of **1a**−**c** were obtained in CH_3CN + 0.1 M TBAP by cyclic voltammetry and by rotating-disk electrode (RDE) experiments. The oxidized forms (**2a**−**c** and **3a**−**c**) were generated stepwise by exhaustive electrolyses and characterized by UV−visible and EPR spectroscopies. Because the potentials of the reversible oxidation of the parent complexes $[Ru(bpy)_2(L_n)]^{2+}$ and $[Mn_2O_2(dmbpy)_4]^{3+}$ are close together ($\Delta E_{1/2}$ = 0.05 V, with the binuclear Mn complex being more easily oxidized than the Ru subunits; see Table 2), the precise

Table 1. UV−Visible Data for $[Ru(bpy)_2(L_n)]^{2+}$, $[Mn_2O_2(dmbpy)_4]^{3+}$, and $[Mn_2O_2\{Ru(bpy)_2(L_n)\}_4]^{11+}$ (**1a−c**) in CH_3CN + 0.1 M TBAP

complexes	λ_{abs}/nm (ϵ/M^{-1} cm^{-1})
$[Ru(bpy)_2(L_2)]^{2+}$ [18]	244 (34000), 286 (72000), 354^a (5500), 396^a (5100), 430^a (10300), 454 (12000)
$[Ru(bpy)_2(L_4)]^{2+}$ [18]	244 (31000), 286 (87000), 354^a (5500), 396^a (5200), 430^a (10700), 454 (12300)
$[Ru(bpy)_2(L_6)]^{2+}$ [18]	244 (32000), 286 (86000), 354^a (5700), 396^a (5400), 430^a (11000), 454 (12700)
$[Mn_2O_2(dmbpy)_4]^{3+}$ [10]	406 (2060), 470 *a* (1250), 528 (550), 559 (450), 688 (560)
1a	243 (162000), 287 (283000), 354^a (32500), 396^a (26000), 430^a (50000), 454 (58000), 680 (580)
1b	243 (161500), 287 (388000), 354^a (30000), 396^a (25200), 430^a (50900), 454 (58000), 680 (598)
1c	243 (176000), 287 (333000), 354^a (32200), 396^a (27300), 430^a (51600), 454 (58000), 680 (590)

[a] Shoulder.

Table 2. Electrochemical Data for $[Ru(bpy)_2(L_n)]^{2+}$, $[Mn_2O_2(dmbpy)_4]^{3+}$, and $[Mn_2O_2\{Ru(bpy)_2(L_n)\}_4]^{11+}$ (**1a−c**) in Deoxygenated CH_3CN + 0.1 M TBAP versus Ag/Ag^+ (0.01 M $AgNO_3$ in CH_3CN + 0.1 M TBAP), at a Scan Rate of 100 mV s^{-1}

	oxidation processes		reduction processes			
	$E_{1/2}$/V (ΔE_p/mV)		E_{pc}/V	$E_{1/2}$/V (ΔE_p/mV)^a		
complexes	$Mn_2^{III,IV}/Mn_2^{IV,IV}$	Ru^{II}/Ru^{III}		first	second	third
$[Ru(bpy)_2(L_2)]^{2+}$ [18]		0.910 (60)		−1.665 (50)	−1.855 (50)	−2.105 (50)
$[Ru(bpy)_2(L_4)]^{2+}$ [18]		0.905 (60)		−1.665 (50)	−1.862 (50)	−2.115 (50)
$[Ru(bpy)_2(L_6)]^{2+}$ [18]		0.905 (60)		−1.665 (50)	−1.865 (50)	−2.125 (50)

	oxidation processes		reduction processes			
	$E_{1/2}$/V (ΔE_p/mV)		E_{pc}/V	$E_{1/2}$/V (ΔE_p/mV)^a		
	$Mn_2^{III,IV}/Mn_2^{IV,IV}$	Ru^{II}/Ru^{III}	$Mn_2^{III,IV}/Mn_2^{III,III}$	first	second	third
$[Mn_2O_2(dmbpy)_4]^{3+}$ [10]	0.86 (80)		−0.10			
1a	0.83^b	0.90 (60)	−0.14	−1.64 (80)	−1.83 (100)	−2.11 (100)
1b	0.82^b	0.90 (60)	−0.12	−1.64 (80)	−1.84 (80)	−2.11 (100)
1c	0.82^b	0.90 (80)	−0.12	−1.66 (80)	−1.85 (90)	−2.11 (100)

[a] Ligand-centered reduction processes. [b] Potentials determined by RDE experiments.

determination of the oxidation potentials of each subunit of **1** is difficult.

The cyclic voltamogramms exhibit only a single couple of anodic and cathodic peaks even at a slow scan rate (v = 20 mV s^{-1}). RDE experiments are more informative. A first wave attributed to the one-electron oxidation of the $Mn_2^{III,IV}$ system is detected as a shoulder at the foot of the main wave relative to the four-electron oxidation of the Ru units (Figure 4B, curve a). The height of this overall five-electron wave versus that of the free Ru complex (4 times more concentrated) is in the ratio 5:4 (Figure 4B, curve b). Although the exact limiting current values of both electrochemical processes cannot be accurately determined, the measurement of the $E_{1/2}$ value of each part of the RDE curve allows one to give an estimation of the redox potentials of the $Mn_2^{IV,IV}$/$Mn_2^{III,IV}$ and Ru^{III}/Ru^{II} systems (see Table 2). The difference between the two couples was found to be around 80 mV instead of 50 mV for the nonconnected molecular systems, indicating that the reaction between the Ru^{III} moieties and the $Mn_2^{III,IV}$ core should be exergonic. In the negative area, three successive ligand-centered reduction reversible systems are observed on the cyclic voltammogram, with an additional typical low-intensity irreversible $Mn_2^{III,IV}$/ $Mn_2^{III,III}$ reduction peak at E_{pc} = −0.12 to −0.14 V (eq 8, Figure 4A, and Table 2). It should be noted that the length of the aliphatic bridges of the L_n ligands has no significant effect on the potential values of the oxidative and reductive processes.

$$[Mn_2^{III,IV}O_2\{Ru^{II}(bpy)_2(L_n)\}_4]^{11+} \underset{b}{\overset{a}{\rightleftarrows}} [Mn_2^{IV,IV}O_2\{Ru^{II}(bpy)_2(L_n)\}_4]^{12+} + e^- \quad (6)$$

$$[Mn_2^{IV,IV}O_2\{Ru^{II}(bpy)_2(L_n)\}_4]^{12+} \underset{b}{\overset{a}{\rightleftarrows}} [Mn_2^{IV,IV}O_2\{Ru^{III}(bpy)_2(L_n)\}_4]^{16+} + 4e^- \quad (7)$$

$$[Mn_2^{III,IV}O_2\{Ru^{II}(bpy)_2(L_n)\}_4]^{11+} + e^- \rightarrow [Mn_2^{III,III}O_2\{Ru^{II}(bpy)_2(L_n)\}_4]^{10+} \quad (8)$$

The two oxidized forms of the complexes, $[Mn_2^{IV,IV}O_2\{Ru^{II}(bpy)_2(L_n)\}_4]^{12+}$ (**2a−c**) and $[Mn_2^{IV,IV}O_2\{Ru^{III}(bpy)_2(L_n)\}_4]^{16+}$ (**3a−c**), can be obtained with a fairly good yield

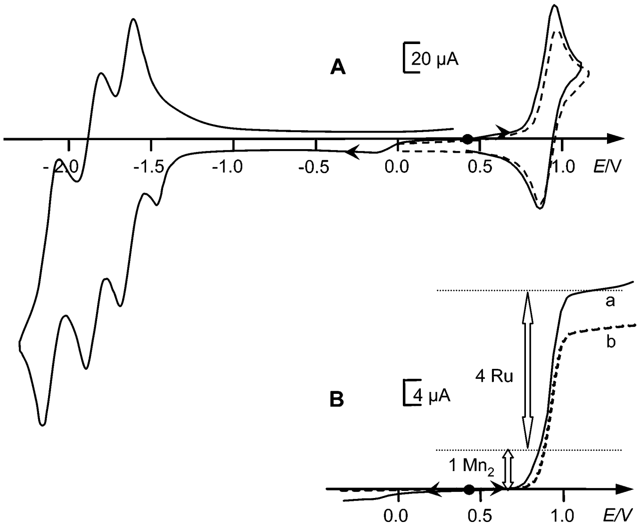

Figure 4. (A) Cyclic voltammograms of solutions of **1c** (0.46 mM, bold line) and $[Ru(bpy)_2(L_6)]^{2+}$ (1.84 mM, dotted line) in CH_3CN + 0.1 M TBAP at a Pt electrode (scan rate: 100 mV s^{-1}). (B) Voltammograms at a Pt RDE at ω = 600 tr min^{-1} (scan rate 10 mV s^{-1}) of (a) a solution of **1c** (0.46 mM) and (b) a solution of $[Ru(bpy)_2(L_6)]^{2+}$ (1.84 mM) in CH_3CN + 0.1 M TBAP.

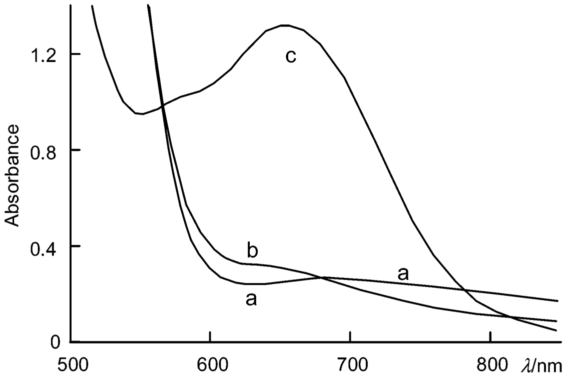

Figure 5. Absorption spectra of a 0.46 mM solution of **1c** in CH_3CN + 0.1 M TBAP: (a) initial solution; (b) after electrolysis at 1.0 V (one electron consumed), formation of **2c**; (c) after exhaustive electrolysis at 1.0 V (four additional electrons consumed), formation of **3c** ($l = 1$ cm).

by two sequential electrolyses at $E = 1.0$ V (one and four electrons consumed per molecule of initial **1a**−**c**, respectively) as judged by spectroscopic titration experiments (UV−visible and X-band EPR). These oxidation processes are associated with significant changes in the visible absorption spectra. The formation of **2a**−**c** is evidenced by the emergence of a large band centered at 644 nm (oxo to Mn^{IV} charge-transfer band) at the expense of the initial absorption band at 680 nm of **1a**−**c** (Figure 5). The other higher energy visible bands expected for the $Mn_2^{IV,IV}$ subunits (shoulders that appear at 570, 465, and 420 nm for $[Mn_2^{IV,IV}O_2(dmbpy)_4]^{3+}$)[10] are masked by the intense Ru^{II} absorption bands. The intensity of the visible band at 454 nm remains unchanged, indicating that the Ru^{II} units are not oxidized (Figure S1 in the Supporting Information). Determination of the accurate yield of the electrogenerated species **2a**−**c** spectroscopically in the wavelength region 600−750 nm is, however, difficult.

A high yield of the oxidized forms is confirmed by EPR spectroscopy (Figure 2). After passage of 1 C per **1a**−**c**, the 16-line EPR signal of the $Mn_2^{III,IV}$ part centered at $g = 2.0$ almost completely disappears, as is expected for the formation of the EPR-silent $Mn_2^{IV,IV}$ moiety, while only a very small signal of the paramagnetic Ru^{III} species is detected at $g = 2.7$[10] (Figure 2b). As judged by the relative intensity of the EPR signals, a **2a**−**c** formation yield higher than 90% has been determined. This percentage is in close agreement with the disproportionation constant obtained from $\Delta E_{1/2}$ of the $Mn_2^{IV,IV}/Mn_2^{III,IV}$ and Ru^{III}/Ru^{II} couples. Further electrolysis allows the formation of **3a**−**c**, which induces a drastic change in color of the solution from orange to pale green due to the disappearance of the visible bands of the Ru^{II} units and the appearance of the characteristic bands of the Ru^{III} species ($\lambda = 428$ and 656 nm; Figure S1 in the Supporting Information). It should be noted that a shoulder at 580 nm typical of the $Mn_2^{IV,IV}$ unit is now detectable, while its band centered at 644 nm is masked by the 656 nm Ru^{III} band. On the basis of the ϵ value of the Ru^{III} species at 656 nm (i.e., 635 M^{-1} cm^{-1} for $[Ru^{III}(bpy)_2(L_6)]^{3+}$)[10] and the absorbance of the binuclear $Mn_2^{IV,IV}$ core at this wavelength, the yield of **3a**−**c** may be determined more accurately. We found a yield value close to quantitative (i.e., >85%). Moreover, this oxidation step, when followed by EPR, leads to observation of the signal corresponding to the Ru^{III} subunits only.[10]

We have also verified that the fully oxidized species **3a**−**c** can be reduced to their initial forms **1a**−**c** (eqs 7b and 8b) by exhaustive electrolyses at $E = 0.7$ V (five electrons consumed per molecule of the hexanuclear complex). The cyclic voltammograms and UV−visible spectra obtained are superimposable with the initial ones. This indicates, in particular, that no decomposition of the **3a**−**c** and **2a**−**c** species occurs during the electrochemical processes.

Table 3. Photophysical Data Determined in a Deoxygenated Solution of $[Ru(bpy)_3]^{2+}$, $[Ru(bpy)_2(L_n)]^{2+}$, and $[Mn_2O_2\{Ru(bpy)_2(L_n)\}_4]^{11+}$ (**1a**−**c**) in CH_3CN + 0.1 M TBAP at 25 °C

complexes	λ_{emis} [nm]	τ [μs]	ϕ	k_r [s^{-1}][b]
$[Ru(bpy)_3]^{2+}$ [18]	603	1.06	0.062	5.8×10^4
$[Ru(bpy)_2(L_2)]^{2+}$ [18]	611	1.11	0.060	5.4×10^4
$[Ru(bpy)_2(L_4)]^{2+}$ [18]	612	1.12	0.054	4.8×10^4
$[Ru(bpy)_2(L_6)]^{2+}$ [18]	612	1.13	0.059	5.2×10^4
1a	613	0.93[a]	0.046	4.9×10^4
1b	613	0.93[a]	0.046	4.9×10^4
1c	613	0.92[a]	0.048	5.2×10^4

[a] Determined for a 5×10^{-6} M concentration. [b] Radiative rate constant $k_r = \phi/\tau$.

Emission. Photophysical studies in CH_3CN + 0.1 M TBAP show that in **1a**−**c** the excited-state energy and electronic structure of the Ru^{II} subunits are not affected by their attachment to the $Mn_2^{III,IV}$ center. The maximum emission wavelengths of the metal-to-ligand CT (MLCT) triplet state of **1a**−**c** and $[Ru(bpy)_2(L_n)]^{2+}$ are similar ($\lambda_{emis}^{max} = 613 \pm 1$ nm), as are the radiative rate constants ($k_r = \phi/\tau$; Table 3). For a 5×10^{-6} M concentration, the luminescence quantum yields of **1a**−**c** (ϕ) and the lifetimes of their excited states (τ) are lower than those of the Mn-free complex $[Ru(bpy)_2(L_n)]^{2+}$ (Table 3),[18] indicating a partial quenching of the luminescence of the Ru^{II} centers in **1a**−**c**. The steady-state emission is moderately quenched, 23−15% depending to the complex involved. However, for very dilute solutions, values of τ and ϕ are very close to those of the parent Mn-free $[Ru(bpy)_2(L_n)]^{2+}$ complex [i.e., $\tau = 1.12$ μs; $\phi = 0.058$ for **1c** (10^{-6} M)]. The emission decays of the hexanuclear complexes are in each case single exponential, showing that no dissociation process, like, for instance, the release of the $[Ru(bpy)_2(L_n)]^{2+}$ subunits associated with the destruction of the $Mn_2^{III,IV}O_2$ core, occurs as a function of the concentration.

A similar situation has already been reported for a series of heterobinuclear complexes of Ru and Fe, $[Ru^{II}(bpy)_2(L_n)Fe^{II}(bpy)_2]^{4+}$ ($n = 2, 4, 6$), in which τ decreases as the concentrations of the complexes increase.[18] In those complexes, the quenching occurs mainly by an energy-transfer process and has been attributed, in part, to an electron-exchange process from the Ru^{II*} unit to the Fe^{II} one, completed by a trivial radiative transfer in which the luminescence of the Ru^{II*} unit is partially reabsorbed by the Fe^{II} unit. For the hexanuclear **1a**−**c** complexes, the situation

---

(18) Lafolet, F.; Chauvin, J.; Collomb, M.-N.; Deronzier, A.; Laguitton-Pasquier, H.; Leprêtre, J.-C.; Vial, J.-C.; Brasme, B. *Phys. Chem. Chem. Phys.* **2003**, *5*, 2520.

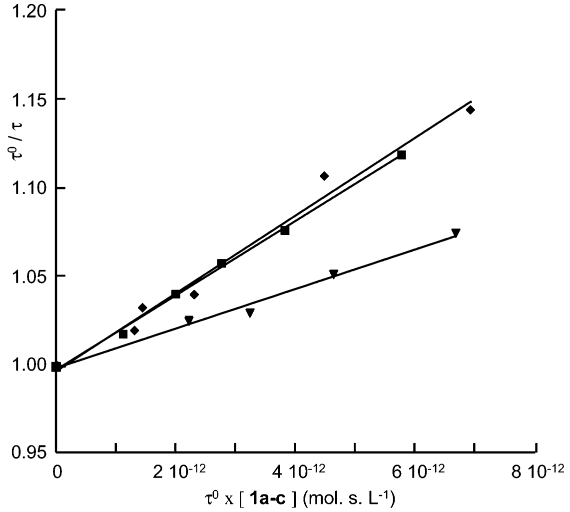

Figure 6. Stern−Volmer plots in deoxygenated CH_3CN for **1a**−**c**: **1a** (▼); **1b** (◆); **1c** (■).

is more complicated because , as was previously reported for the parent bimolecular $[Ru(bpy)_3]^{2+}/[Mn_2O_2(dmbpy)_4]^{3+}$ system, the quenching of $[Ru(bpy)_3]^{2+}*$ by $[Mn_2O_2(dmbpy)_4]^{3+}$ can occur following two different processes.[10] The first is an energy-transfer process and the second an oxidative process by an electron transfer involving the reduction of the $Mn_2^{III,IV}$ core. However, we found in this system that, for thermodynamic and kinetic reasons, the energy transfer presumably represents the main contribution to the quenching process of $[Ru(bpy)_3]^{2+}*$ by the binuclear Mn oxo complex. So, the variation of the lifetime τ according to the **1a**−**c** concentration could be due to some intermolecular quenching. To estimate the quenching rate (k_{EN}) for these hexanuclear complexes, a Stern−Volmer equation based on the luminescence lifetime measurements, the luminescence lifetime of $[Ru(bpy)_2(L_n)]^{2+}$ as τ_0, and the dependence of τ vs [**1a**−**c**] as the variable has been used (eq 9 and Figure 6).

$$\tau_0/\tau = 1 + k_{EN}\tau_0[\mathbf{1a}-\mathbf{c}] \qquad (9)$$

Surprisingly, the k_{EN} values for the three hexanuclear complexes lie in the range (1−2) × 10^{10} L mol^{-1} s^{-1} with only a slight influence of the methylene bridge length and close to the diffusion limit rate constant of the molecules. It should be recalled that, for the bimolecular system $[Ru(bpy)_3]^{2+}/[Mn_2O_2(dmbpy)_4]^{3+}$, the quenching rate was only 2.5×10^9 L mol^{-1} s^{-1} and presumably attributed to an energy transfer by an exchange mechanism. In such a process, molecules need to diffuse in order to overlap their electron clouds. Of course, other phenomena like self-quenching of the four Ru^{II} subunits or triplet−triplet annihilation cannot be ruled out. At this stage of this study, the exact nature of the quenching process remains unclear. Further experiments like time-correlated single photon counting will be needed to further investigate this process.

Photoinduced Electron Transfer. The energy-transfer process between the $Ru^{II}*$ and $Mn_2^{III,IV}O_2$ units can easily be short-circuited by the addition of the external irreversible electron acceptor (4-bromophenyl)diazonium tetrafluoroborate ($ArN_2^+BF_4^-$). We have previously demonstrated that, for a mixture of $[Ru^{II}(bpy)_3]^{2+}$ and $[Mn_2^{III,IV}O_2(dmbpy)_4]^{3+}$, ArN_2^+ reacts preferentially with the excited-state $[Ru^{II}(bpy)_3]^{2+}*$ and leads to $[Ru^{III}(bpy)_3]^{3+}$, which plays the role of an oxidant toward $[Mn_2^{III,IV}O_2(dmbpy)_4]^{3+}$.[10] As a consequence, continuous irradiation leads to the formation of $[Mn_2^{IV,IV}O_2(dmbpy)_4]^{4+}$ in nearly quantitative yield. For **1a**−**c**, a similar efficient photogeneration of the corresponding Ru^{III} species, i.e., $[Mn_2^{III,IV}O_2\{Ru^{III}(bpy)_2(L_n)\}\{Ru^{II}(bpy)_2(L_n)\}_3]^{12+}$, is expected (eq 10).

Scheme 1 . Schematic Representation of the Photooxidation Mechanism of **1a**−**c** in the Presence of an External Electron Acceptor (ArN_2^+)

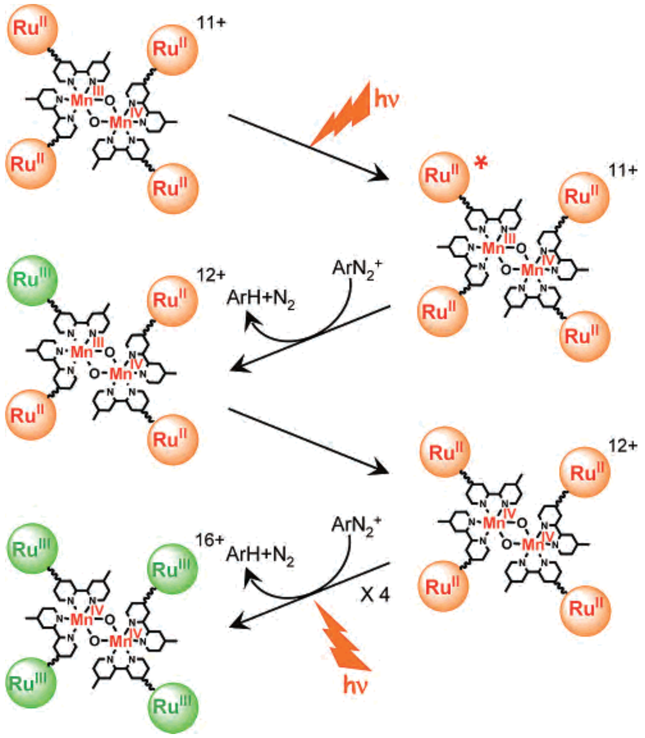

$$[Mn_2^{III,IV}O_2\{Ru^{II*}(bpy)_2(L_n)\}\{Ru^{II}(bpy)_2(L_n)\}_3]^{11+} + ArN_2^+ \xrightarrow{k_{ET}} [Mn_2^{III,IV}O_2\{Ru^{III}(bpy)_2(L_n)\}\{Ru^{II}(bpy)_2(L_n)\}_3]^{12+} + ArN_2^{\bullet} \qquad (10)$$

The rate constants of the oxidative quenching (k_{ET}) of the excited states of **1a**−**c** by ArN_2^+ were determined from the Stern−Volmer plot (eq 11), where τ and τ_{Ar} are the

$$\tau/\tau_{Ar} = 1 + k_{ET}\tau[ArN_2^+] \qquad (11)$$

luminescence lifetimes of **1a**−**c** without and with a variable concentration of ArN_2^+ (0.05−1 mM), respectively, and k_{ET} is the rate constant of the electron-transfer reaction according to eq 10. k_{ET} values obtained for **1a**−**c** of about 4.0×10^9 M^{-1} s^{-1} show no influence of the L_n chain length and are very similar to that of the $[Ru^{II}(bpy)_3]^{3+}/ArN_2^+$ system.[9] These high values of k_{ET} illustrate that the photogeneration of $[Ru^{III}(bpy)_3]^{3+}$ is highly efficient.

Photooxidation by Continuous Irradiation. Solutions of **1a**−**c** (∼0.45 mM) in the presence of an excess of ArN_2^+

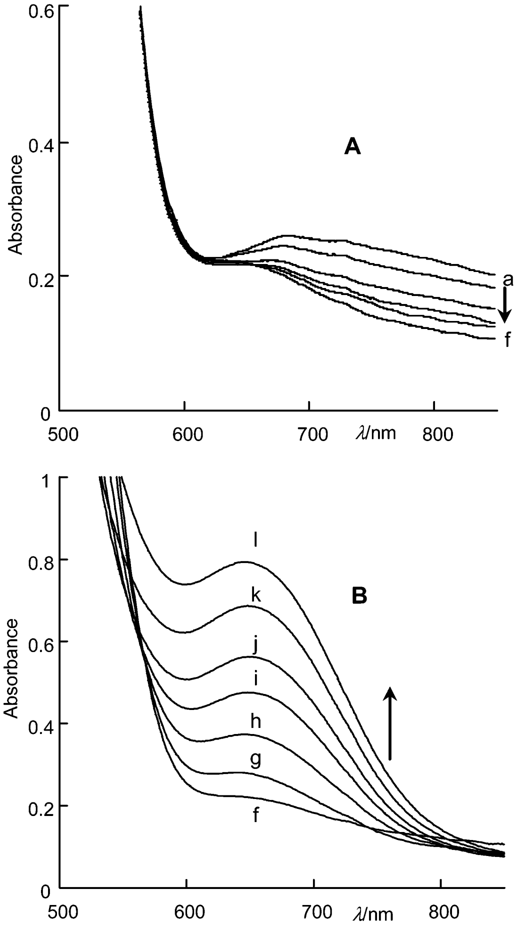

Figure 7. Visible absorption spectral change of a $CH_3CN + 0.1$ M TBAP solution of **1c** (0.44 mM) and ArN_2^+ (15 mM) under visible irradiation: (A) (a) initial; (b) after 2 min 30 s; (c) 5 min 30 s; (d) 7 min 40 s; (e) 10 min 10 s; (f) 17 min 10 s (formation of 80% of **2c**). (B) (f) 17 min 10 s; (g) 25 min 15 s; (h) 44 min 30 s; (i) 59 min; (j) 77 min; (k) 110 min; (l) 258 min; $l = 1$ cm.

(15 mM) in $CH_3CN + 0.1$ M TBAP were continuously irradiated with a mercury or xenon lamp whose IR and UV radiation are cut off (see the Experimental Section). Successive photogenerations of **2a−c** and **3a−c**, as illustrated in Scheme 1, were followed by UV−visible absorption.

Two successive changes of the absorption spectra were observed during the irradiation (Figure 7). In the first step, a progressive emergence of the shoulder at 644 nm at the expense of the visible absorption band at 680 nm is observed, consistent with the formation of **2a−c** via the transient photogenerated Ru^{III} species. The **2a−c** formation yields are close to 80% (estimated by spectroscopic titration) and are reached after about 20 min of irradiation (Figure 7, spectrum f), demonstrating the efficiency of the photoinduced oxidation processes. These results confirm that the Ru^{III} species is an efficient oxidant toward the $Mn_2^{III,IV}$ core. Continued irradiation induces the formation of **3a−c**, as illustrated by the intense LMCT band of the Ru^{III} unit at 656 nm (Figure 7B, spectrum l). In addition, operating with more dilute solutions, as expected, this oxidative step is also displayed by the decrease of the MLCT band of the Ru^{II} unit at 454 nm and the appearance of two new bands at 428 and 656 nm, typical of the Ru^{III} species (Figure S2 in the Supporting Information). Irradiations have been stopped arbitrarily when about 60% of the Ru^{III} species is reached.

The **2a−c** yield is slightly lower than that obtained by electrochemical oxidation, as a consequence of a slow photoinduced degradation of the $Mn_2^{III,IV}$ or $Mn_2^{IV,IV}$ moieties of the hexanuclear complexes during irradiation as previously reported for irradiation experiments carried out with a simple mixture of $[Ru^{II}(bpy)_3]^{2+}$ and $[Mn_2^{III,IV}O_2(dmbpy)_4]^{3+}$.[10] In addition, the quantum yield of the overall photoinduced oxidation for **2a** has been estimated. Its value (0.15 ± 0.05) is modest and in good agreement with the quantum yield of the photoproduction of Ru^{III} species using (4-bromophenyl)-diazonium salt as the quencher ($\phi = 0.34^{14}$), with this process being a major limiting factor of the overall process. Finally, it appears that the length of the alkyl chain has no decisive influence on the yield and on the rate of formation of **2a−c** and **3a−c**.

Conclusion

We have synthesized three poly(bipyridyl) hexanuclear complexes consisting of one $Mn_2^{III,IV}(\mu\text{-}O)_2(dmbpy)_4$-type subunit covalently linked to four photoactive $Ru^{II}(bpy)_3$ moieties. These complexes represent unusual examples of Mn complexes having $(\mu\text{-}O)_2$ bridges linked to photoactive units, similar to the natural Mn cluster. We have shown that, in these complexes, a partial quenching of the MLCT excited state of the Ru^{II} centers by the $Mn_2^{III,IV}$ unit occurs, with its exact nature remaining elusive. However, this energy-transfer process can be easily short-circuited in the presence of an external irreversible electron acceptor by an electron transfer allowing the photoinduced formation of Ru^{III} subunits, which, in turn, oxidize the $Mn_2^{III,IV}$ moiety into the stable $Mn_2^{IV,IV}$ species.

We show here for the first time that it is possible to induce, with a good overall efficiency, the oxidation of a $Mn_2(\mu\text{-}O)_2$ core in a heterobimetallic Mn−Ru complex photochemically.

Acknowledgment. The authors are grateful to the Centre de Recherches du Service de Santé des Armées “Emile Pardé”, Laboratoire de Biospectrométrie, La Tronche, France, for ESI-MS experiments.

Supporting Information Available: Evolution of the visible absorption spectra of **1c** (0.275 mM) during electrolysis ($l = 1$ mm) (Figure S1) and visible absorption changes of **1c** (0.055 mM) under irradiation ($l = 1$ cm) (Figure S2). This material is available free of charge via the Internet at http://pubs.acs.org.

IC0624726